Applied Radiation and Isotopes 231 (2026) 112521

Contents lists available at ScienceDirect

Applied Radiation and Isotopes

journal homepage: www.elsevier.com/locate/apradiso

MEYER project: Towards a national protocol for in vivo measurement of ^{131}I in the thyroid of exposed populations in emergencies

J.F. Navarro [a,*], B. Pérez [a], M.A. López [a], S. Pereira [b], J. Ruiz [c], I. Sierra [a], D. Rueda [b], I. Villanueva [b]

[a] CIEMAT, Center for Energy, Environmental, and Technological Research, Madrid, Spain
[b] CSN, Nuclear Safety Council, Madrid, Spain
[c] TECNATOM -Westinghouse Electric Company, Madrid, Spain

ARTICLE INFO

Keywords:
Gamma spectrometry with germanium detectors
In-vivo monitoring of I-131 in thyroid
Age-dependent thyroid phantoms
Nuclear or radiological emergencies
Thyroid monitoring
Calibration phantoms for children and adults

ABSTRACT

The "MEYER" project (Protocolo Nacional para la MEdida de Yodo en tiroides en Emergencias Radiológicas), initiated by Spain's National R&D Platform for Radiological Protection (PEPRI), aims to enhance national capabilities for the rapid screening of the exposed population to iodine-131 (^{131}I) during nuclear or radiological emergencies. Its primary objective is to address challenges in quantifying internal thyroid contamination in large-scale emergencies, where internal dosimetry services may became overwhelmed.

The project is structured into three phases. In phase 1, age-dependent thyroid phantoms representing children (aged 1, 5, and 10 years old) and adults were developed. Each phantom incorporated a vial with a radioactive solution of ^{133}Ba and ^{137}Cs to simulate ^{131}I contamination. A calibration protocol for both spectrometric and non-spectrometric devices was established, followed by an intercalibration campaign involving seven entities and the calibration of their own devices. Phase 2 focused on validating these protocols through the organization of an intercomparison campaign at selected centres, including hospitals, dosimetry services and military units. Finally, phase 3 involves the project's conclusion and the dissemination of results.

This study presents the findings from the intercalibration campaign (Phase 1). Preliminary results indicate that counting efficiency values for most calibrated devices decreases with the age-dependent phantom type, with variations reaching up to 60%. Gamma cameras showed high detection sensitivity, making them suitable for large-scale screening in emergencies. On the other hand, surface contamination monitors and radiometers present lower sensitive compared to gamma cameras. These findings highlight the importance of leveraging existing equipment to enhance emergency management strategies.

1. Introduction

Quantifying the intake of iodine-131 (^{131}I) in the thyroid of individuals of the exposed population is one of the primary concerns to take into account in nuclear or radiological emergencies (UNSCEAR, 2013). In such scenarios, a rapid screening of exposed individuals is required to assess their level of internal contamination and to establish appropriate action protocols and countermeasures. (Broggio et al., 2019). Direct in-vivo measurement of ^{131}I in thyroid is the recommended technique for assessing intakes. This can be accomplished using spectrometric instruments commonly equipped with either sodium iodide scintillation detectors or germanium detectors (Perez et al., 2020). On the other hand, in situations involving large numbers of exposed individuals, the capacity of authorized internal dosimetry services may become overwhelmed, necessitating external support from other institutions or organizations equipped with calibrated devices and appropriate operational protocols for performing such type of measurements.

To address this challenge, the MEYER project was initiated within the framework of the National R&D Platform for Radiological Protection (PEPRI) from Spain. The project is based on a scientific collaboration agreement between the Nuclear Safety Council (CSN) as the regulatory authority, CIEMAT as a public research organization, and TECNATOM-Westinghouse as a representative of the nuclear industry.

This article is part of a special issue entitled: Reprolam 2024 published in Applied Radiation and Isotopes.

* Corresponding author. Research Centre for Energy Environment and Technology, Madrid, Madrid, Spain.
E-mail address: jf.navarro@ciemat.es (J.F. Navarro).

https://doi.org/10.1016/j.apradiso.2026.112521
Received 27 January 2025; Received in revised form 27 November 2025; Accepted 10 February 2026
Available online 19 February 2026
0969-8043/

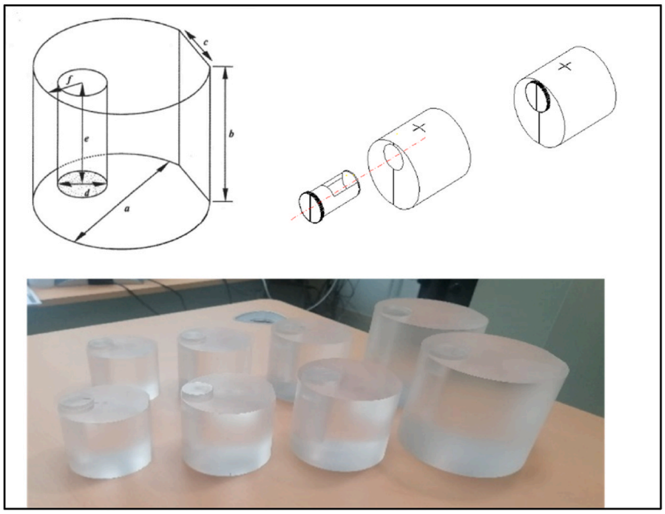

Fig. 1. Adult male; 10-year-old, 5-year-old and 1-year-old child thyroid-neck phantom.

Table 1
Dimensions: adult and children thyroid phantoms.

Age- dependent Thyroid phantom	Perimeter (mm)	φ diameter (mm)	Thyroid Volume (ml)	Overlying tissue Thickness (mm)
1- year-old	220 ± 2	71,0 ± 0,5	1.7	2,1 ± 0,5
5- year-old	260 ± 3	82,0 ± 0,5	3.2	3,0 ± 0,5
10- year-old	300 ± 4	95,0 ± 0,5	7.5	4,2 ± 0,5
Adult male	410 ± 5	127,0 ± 0,5	19.0	5,0 ± 0,5

The main objective of the project is to develop a national protocol for the determination of ^{131}I activity in the thyroid of exposed population during radiological or nuclear emergencies. This includes adapting national capabilities for the rapid screening of individuals with internal contamination in scenarios involving a large number of potentially exposed individuals. In this way, the response capacity to nuclear or radiological emergencies is enhanced, thereby contributing to public safety in such situations.

The MEYER project is structured into three phases to address the critical need for efficient and accurate internal dosimetry during radiological emergencies. **Phase 1** involved the fabrication of age-dependent thyroid phantoms representing adults and children aged 1, 5, and 10 years. These phantoms were designed to incorporate radioactive solutions of ^{133}Ba and ^{137}Cs in a suitable proportion for simulating the spectrum of ^{131}I. This ratio changes over time due to the considerably different half-lives of ^{133}Ba (10 years) and ^{137}Cs (30 years). However, this variation can be considered negligible because the calibrations were performed over short time intervals. Furthermore, a calibration protocol was developed for both spectrometric and non-spectrometric equipment, with specific recommendation for gamma cameras. This phase also included an intercalibration involving CIEMAT, TECNATOM-Westinghouse, and other collaborating institutions with expertise in the handling and calibration of these device. **Phase 2,** currently in progress, is focused on the verification and validation of the protocol and methodologies established in the first phase. This is being achieved through a comprehensive intercalibration and intercomparison campaign conducted at selected centres. These centres include facilities equipped to provide support during the early stages of a radiological emergency, such as authorized dosimetry services, radiological protection units, hospitals, and military emergency response teams. Finally, **Phase 3** will conclude the project by compiling the findings and disseminating the results, thereby enhancing national capabilities for managing radiological emergencies.

2. Organization of the intercalibration exercise: phase 1

2.1. Calibration protocol

In order to harmonize calibration procedures for different kinds of equipment used in nuclear or radiological emergencies and to establish a robust protocol for ^{131}I thyroid measurements during the early phase of such scenarios, various calibration geometries were proposed, distinguishing three categories of equipment: spectrometric devices, non-spectrometric devices, and gamma cameras. In all cases, the calibration geometry must be reproducible and realistic for emergency conditions, ensuring subject comfort, system stability, and short measurement times. The equipment was classified according to the three categories of the protocol to enable a more comprehensive analysis of the results.

2.1.1. Non-spectrometric devices

In case of non-spectrometric devices, the protective window should be removed, and the thyroid-neck phantom positioned vertically. The measurement device must be aligned vertically in front of the phantom, ensuring the detector window is centred on the thyroid region. Calibrations will be conducted at two phantom-detector distances: 5 cm and 10 cm. Prior to calibration measurements, a background measurement is recommended to calculate the calibration factor by subtracting the contribution of ambient radiation. This involves first measuring background counts with the blank phantom (without radioactive sources), followed by measuring counts with the active phantom.

2.1.2. Gamma cameras

For calibration measurements with gamma cameras, the collimator should be removed, and the thyroid-neck phantom positioned horizontally (lying down). The detector will be centred over the vial of the thyroid-neck phantom. An energy window will be applied around the main emission of ^{131}I. Calibration measurements will be performed at two phantom-detector distances: 10 cm and 15 cm. Prior to the calibration measurements, background counts should be measured with the blank phantom. Then, counts will be measured with the active phantom and the background counts will be subtracted from the measured values to obtain the net counts.

2.1.3. Spectrometric devices

For spectrometric equipment, the thyroid-neck phantom should be positioned either vertically or horizontally, depending on the standard measurement geometry. The detector will be placed over the centre of the thyroid simulator at the calibration distance. Calibration measurements will be conducted at two "neck-thyroid"-detector distances: 5 cm and 10 cm. If the device has unique characteristics preventing measurements at these distances, the actual measurement distance should be reported. The Region of Interest should be defined centred on the main energy of ^{133}Ba (356 keV). Background counts should be measured with the blank phantom, followed by measurements with the active phantom.

2.1.4. Efficiency and sensitivity of detection for in vivo measurement of ^{131}I in thyroid

For each device, calibration measurements should be performed following the previously mentioned protocol in order to calculate the detection efficiency. The efficiency (Ef), expressed in cps·Bq^{-1}, is the ratio between the net count rate, N (cps), and the decay corrected activity, Aref (Bq), of the calibration source (vials with ^{133}Ba and ^{137}Cs as

Table 2
Participating institutions and their measurement equipment.

Institution	Measurement equipment	Type	
Whole Body Counter Laboratory CIEMAT	Broad energy Germanium detector. Area: 6500 mm2; Diameter: 91.2 mm. Energy range: (10 – 2000 keV. Additional information: https://assets-mirion.mirion.com/prod-20220822/cms4_mirion/files/pdf/spec-sheets/bege-data-sheet.pdf	spectrometric device	
	FASTSCAN whole body counter 2 NaI(Tl) detectors 4″x4″x16". Diameter 91.2 mm. Energy range (100-2000 keV) Shielded in all straight-line directions by 10 cm (4 in.) of low background steel. Additional information: https://tecnasa.es/monitores-de-contaminacion-personales-cuerpo-entero-fastscan-modelo-2250/	spectrometric device	
	Berthold LB 124 Area: 150 cm^2. Detector 100 × 150mm Xenon gas. Proportional counter. Additional information: https://tecnasa.es/desclasificacion-medida-para-radiactividad-en-materiales-de-excavacion-lb-124-scint-d/	non-spectrometric device	
Whole body Counter Laboratory TECNATOM	HELGESON QUICKY whole body counter. NaI(Tl) scintillator detector Diameter: 203 mm; Energy range: (50 Kev- 2 Mev). Additional information: https://helgeson.es/quicky-whole-body-counter-for-internal-dosimetry	spectrometric device	
	HELGESON DYIS. whole body counter. NaI(Tl) scintillator detector Diameter: 203 mm; Energy range: (50 Kev- 2 Mev). Additional information: https://helgeson.es/diys-bed-type-whole-body-counter-for-internal-dosimetry	spectrometric device	
Hospital "la Santa Creu i Sant Pau"	CAPINTEC, CAPTUS 2000 NaI(Tl) scintillation detector 5.1 cm × 5.1 cm(10 Kev a 2 MeV). Additional information: https://www.mirion.com/about/medical/capintec	spectrometric device	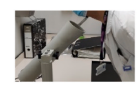
	SIEMENS, Symbia Intevo Bold FOV: 53.3 cm × 38.7 cm Energy range: 35 Kev to 588 Kev. Additional information: https://www.siemens-healthineers.com/molecular-imaging/spect-ct-scanners/symbia-intevo-bold	spectrometric device	
	PHILIPS, Bright View XCT 40,6 x 53,9 cm^2 Energy range: from 0 to 920 keV	spectrometric device	
	Berthold LB124 (ScintD) Detector: ZnS: 118 mm × 145 mm Área:170 cm2 Energy range: from 50 Kev to 1,3 MeV https://tecnasa.es/desclasificacion-medida-para-radiactividad-en-materiales-de-excavacion-lb-124-scint-d/	non-spectrometric device	
Hospital "La Fe de Valencia"	PHILIPS, Bright View XCT BV1 40,6 x 53,9 cm^2 Energy range: from 0 to 920 Kev. Additional information: https://www.philips.co.uk/healthcare/product/HC882482/brightview-xct-spectct-system	gamma camera	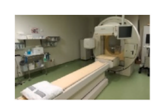
	PHILIPS, Bright View XCT BV2 40,6 x 53,9 cm^2 Energy range: from 0 to 920 Kev https://www.philips.co.uk/healthcare/product/HC882482/brightview-xct-spectct-system	gamma camera	
	NaI(Tl) scintillation detector Canberra MODEL 802. 51 × 51 mm. (crystal size). Energy range: (20 Kev to 3 MeV). Additional information: https://www.mirion.com/products/technologies/spectroscopy-scientific-analysis/gamma-spectroscopy/detectors/scintillation-czt-detectors-accessories/802-scintillation-detectors	spectrometric device	
	MIRION LaBr3(Ce) 1.5″ x 1.5". Diameter:3,81 cm; large: 3.81 cm Energy range: from 50 Kev to 2,8 MeV. Additional information: https://assets-mirion.mirion.com/prod- 0220822/cms4_mirion/files/pdf/spec-sheets/c39490_labr_super_spec_1.pdf	spectrometric device	

(*continued on next page*)

Table 2 (*continued*)

Institution	Measurement equipment	Type	
	CANBERRA Babyline 81 11,5 cm × 29 cm x 23,6 cm (WxDxH)). 1650 g. Energy range from 8 Kev to 10 MeV 515 cm^3 air ionization chamber with 7 mg/cm2 tissue equivalent wall and 300 mg/cm2 removable cap	non-spectrometric device	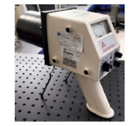
University of Valencia	ORTEC, GEM 201900P (HPGe). Diameter: 56 mm; Large 47 mm Energy range: from 60 keV to 4 MeV.	spectrometric device	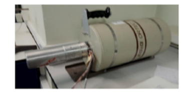
	CANBERRA 51B51 2M (NaI(Tl)). Crystal (2″x2″) 185 mm × 58.8 mm. Energy range: from 50 keV to 4 MeV	spectrometric device	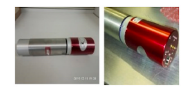
University of Islas Baleares	LAMSE CT15 coupled to LAMSE, MS6020-R Area 15 cm2. Window: Mica 1.5-2 mg/cm^2. Geiger Müller detector 140 mm × 65 mm.	non-spectrometric device	

Table 3
Efficiency values (cps/Bq) – gamma cameras.

EFF (cps/Bq) -Gamma cameras										
EQUIPMENT/INSTITUTION	Tm (s)	CODE	Adult		10y		5 y		1 y	
			10 cm	15 cm	10 cm	15 cm	10 cm	15 cm	10 cm	15 cm
Gamma camera Siemens Hosp Santa Creu y San Pau	300	HSP siemens	3.66E-02	2.77E-02	3.73E-02	2.79E-02	4.02E-02	3.02E-02	4.16E-02	3.08E-02
Gamma camera Philips BV Hosp Santa Creu y San Pau	300	HSP philips	3.78E-02	2.80E-02	3.93E-02	2.90E-02	4.24E-02	3.09E-02	4.89E-02	3.30E-02
Gamma camera Philips BV1 Hosp. La Fe	300	HLaFe philips 1	3.31E-02	2.65E-02	3.37E-02	2.53E-02	3.53E-02	2.75E-02	4.03E-02	2.95E-02
Gamma camera Philips BV2. Hosp. La Fe	300	HLaFe philips 2	3.14E-02	2.40E-02	3.31E-02	2.51E-02	3.49E-02	2.58E-02	3.66E-02	2.73E-02

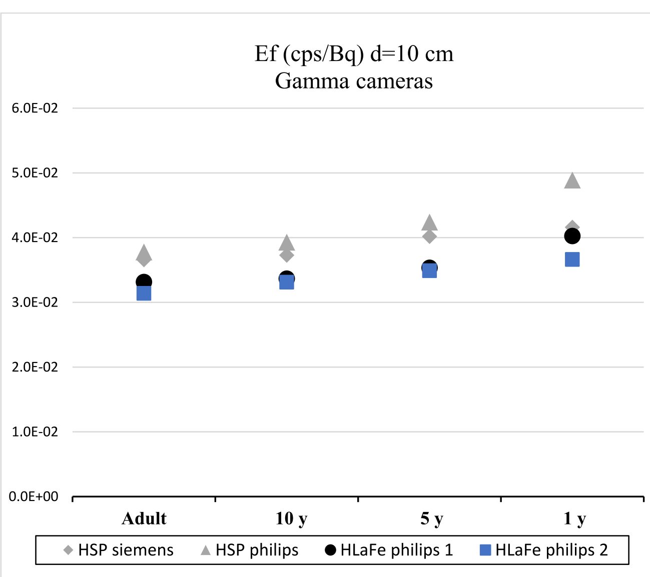

Fig. 2a. Efficiency values for gamma cameras (d = 10 cm).

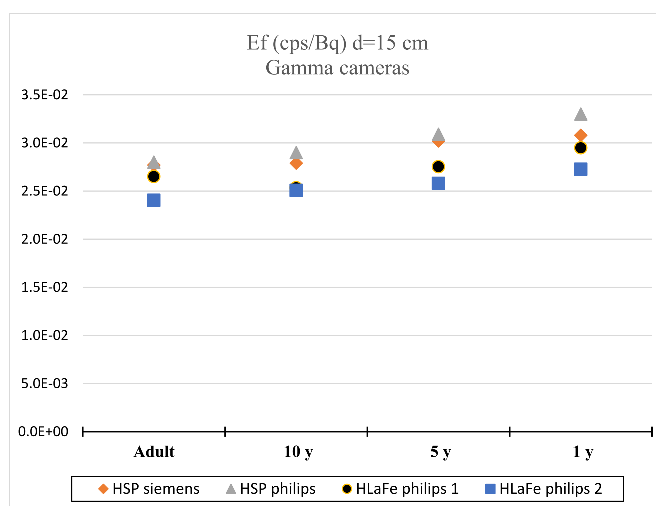

Fig. 2b. Efficiency values for gamma cameras (d = 15 cm).

surrogate of ^{131}I), during the measurement time (Ec1). The reference activity will be corrected for radioactive decay to the date of measurement.

$$Ef\left(\frac{cps}{Bq}\right)\frac{N}{Aref(Bq)}=\frac{[cps]}{[Bq]} \quad \text{(Ec1)}$$

The detection limit (DL) or minimum detectable activity (MDA) defines the ability of a detection system to quantify a radionuclide incorporated by an individual which has been deposited in the whole body or specific organs. The DL or MDA, expressed in Bq, is mainly dependent on

Table 4
Efficiency values (cps/Bq) –Non-spectrometric devices.

EFF (cps/Bq) – non-Spectrometric devices										
EQUIPMENT/INSTITUTION	Tm(s)	CODE	Adult		10y		5 y		1 y	
			10 cm	5 cm	10 cm	5 cm	10 cm	5 cm	10 cm	5 cm
BERTHOLD LB124 CIEMAT	120	CIEMAT LB124	4.6E-03	9.0E-03	5.1E-03	9.7E-03	6.5E-03	1.1E-02	1.0E-02	1.4E-02
BERTHOLD LB124 SCINT D Hosp San Pau	150	HSP LB124	5.9E-03	1.3E-02	6.2E-03	1.4E-02	6.5E-03	1.5E-02	6.7E-03	1.5E-02
LAMSE, MS6020-R. Univ. Islas Baleares	600	UNIV.IB Lamse	1.7E-04	5.9E-05	1.6E-04	6.3E-05	2.1E-04	7.7E-05	2.2E-04	8.3E-05
Babyline 81.ratemeter Univ. País Vasco	60	UPV Babyline		8.4E-06		2.1E-05		2.5E-05		4.6E-05

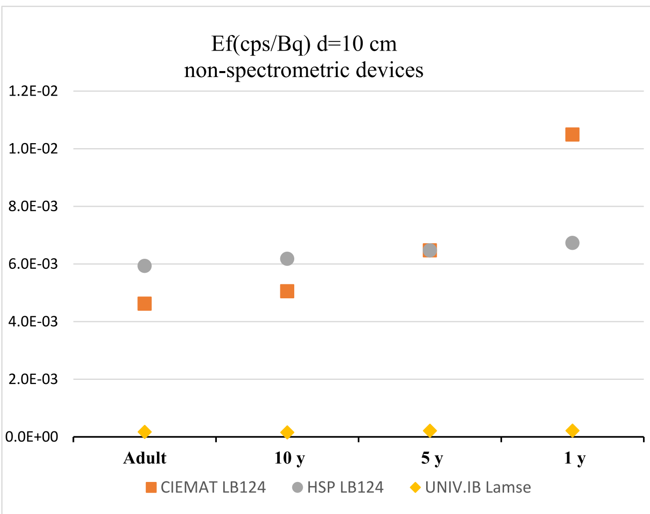

Fig. 3a. Efficiency values for gamma cameras (d = 10 cm).

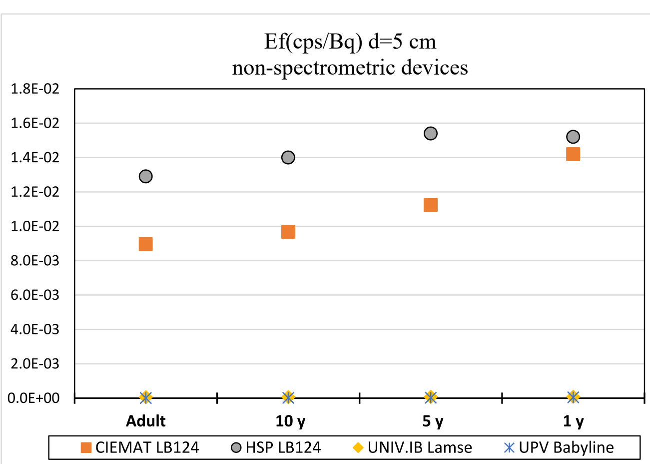

Fig. 3b. Efficiency values for gamma cameras (d = 5 cm).

the person, the measurement geometry, the efficiency and the counting time. To assess detection sensitivity, all participants were provided with blank vials (without radioactive sources) identical to the active ones that will be inserted into the phantoms (blank phantoms). Measurements were conducted under the same geometry and conditions as those used for the calibration measurement. The DLs or MDAs were calculated according to the specific procedure established for each instrument in each laboratory, considering that in this type of scenario (emergencies), short measurement times are recommended to enable rapid population screening.

3. Materials and methods

3.1. Age-dependent thyroid-neck phantoms

CIEMAT has designed and manufactured two families of thyroid-neck phantoms made of polymethyl methacrylate (PMMA), representing different age groups: adult male, 10-year-old child, 5-year-old child, and 1-year-old child. (Fig. 1). The adult phantoms were designed according to ANSI/HPS N13.44-2014 standard (ANSI/HPS N13.44., 2014). Each phantom includes a cylindrical cavity at the top, where a plastic vial simulating the thyroid gland is inserted (Pérez et al., 2020). The vial's volume complies with the recommendations outlined in ICRP Publication 89 (ICRP, 2002). Each vial was filled with a liquid solution containing a known activity of ^{133}Ba and ^{137}Cs (in a 1:0.11 ratio) as a surrogate for ^{131}I. ^{131}I is a fission product with a physical half-life of 8.02 days. Due to its short half-life, the use of an iodine surrogate is recommended in intercomparison exercises.

The dimensions of each thyroid-neck phantom for children were determined based on anthropometric measurements, including neck diameter and the thickness of the thyroid-covering tissue (Pérez et al., 2018). The dimensions of each thyroid-neck phantom are presented in Table 1.

4. Results and conclusions

This article presents the results of the intercalibration campaign (phase I), which involved seven entities and the calibration of 18 devices (Table 2). The participating entities performed the calibration of their devices and determined the efficiency and detection limits for the various proposed geometries, according to the established calibration protocol.

The data on the detection efficiency and sensitivity of the devices have been grouped according to the categories defined in the protocol (spectrometric instruments, non-spectrometric instruments and gamma cameras) in order to facilitate a more comprehensive analysis and to derive conclusions based on the type of measuring instrument. Table 3 shows efficiency values of gamma cameras for each age-specific phantom at detector-phantom distance of 10 cm (Fig. 2a) and 15 cm (Fig. 2b). In the same manner, Table 4 shows efficiency values of non-spectrometric devices (Figs. 3a and 3ba and b). In the case of spectrometric devices (Table 5), not all were able to replicate the geometries defined in the protocol. Therefore, the values have been separated for those that were successfully calibrated at the distances defined in the protocol (Figs. 4a and 4ba and b).

Detection sensitivity was calculated using blank vials that simulate the thyroid gland of a non-contaminated individual. The obtained results were also grouped according to the categories established in the calibration protocol (Tables 6–8).

The primary general conclusion is that counting efficiency values decrease as the age-dependent phantom type increases, with variations reaching up to 60%. This effect is more pronounced when the detector-phantom distance is short (5 cm). These results would justify the use of age-dependent phantoms for a more accurate estimation of internal

Table 5
Efficiency values (cps/Bq) -Spectrometric devices.

Eff (cps/Bq) -Spectrometric devices									
EQUIPMENT/INSTITUTION	CODE	Adult		10 y		5 y		1 y	
		10 cm	5 cm	10 cm	5 cm	10 cm	5 cm	10 cm	5 cm
BEGe detector CIEMAT	CIEMAT BEGe	6.5E-03	1.4E-02	6.8E-03	1.4E-02	7.8E-03	1.7E-02	8.1E-03	1.8E-02
HP Ge detector Univ. VALENCIA	UV HPGe	2.4E-03	5.3E-03	2.5E-03	5.7E-03	2.8E-03	6.4E-03	3.0E-03	7.6E-03
NaI (Tl) detector Univ. VALENCIA	UV NaI	3.1E-03	9.6E-03	3.5E-03	1.0E-02	4.0E-03	1.2E-02	5.0E-03	1.3E-02
NaI (Tl) detector Hosp. La Fe	LaFe NaI	3.3E-03	6.5E-03	2.7E-03	6.8E-03	3.1E-03	7.1E-03	3.2E-03	6.8E-03
LaBr3(Ce) Univ. País Vasco	UPV LaBr3	2.2E-03	5.4E-03	2.4E-03	5.7E-03	2.9E-03	6.8E-03	2.7E-03	8.4E-03
EQUIPMENT/INSTITUTION	CODE	Adult		10 y		5 y		1 y	
		14 cm	25 cm	14 cm	25 cm	14 cm	25 cm	14 cm	25 cm
Quicky NaI counter TECNATOM	TEC_QUICKY	5.1E-03		7.0E-03		1.2E-02		1.2E-02	
FASTSCAN counter CIEMAT	CIEMAT_FS	2.5E-02		2.7E-02		3.0E-02		3.4E-02	
DIYS NaI counter TECNATOM [(1)]	TEC_DIYS	2.1E-02		1.7E-02		1.8E-02		1.7E-02	
CAPTUS2000 Hosp.San Pau	HSP CAPTUS		7.7E-04		7.7E-04		8.4E-04		8.7E-04

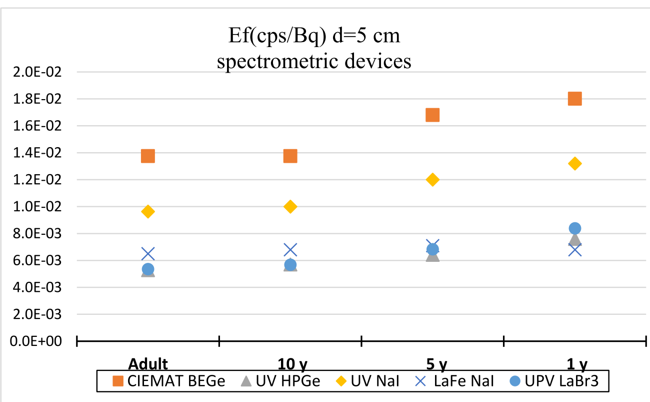

Fig. 4a. Efficiency values for spectrometric devices (d = 5 cm).

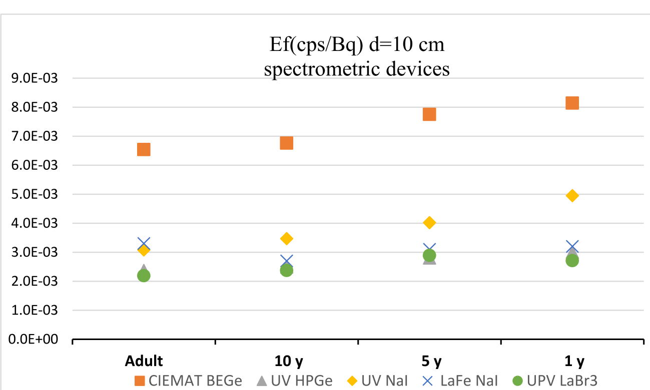

Fig. 4b. Efficiency values for spectrometric devices (d = 10 cm).

doses.

Furthermore, the sensitivity of detection (DL/MDA) decreases with age with variations reaching up 50%. Germanium detectors and gamma cameras present lower values (below 70 Bq) at short measurement time, comparing to other devices (radiometers, surface contamination monitors). On the other hand, NaI(Tl), $LaBr_3$ (Ce) scintillation detectors and surface contamination monitors present moderate values (ranging from 80 to 500 Bq depending on detector-phantom distance and measurement time). Results obtained are in good agreement with other studies (Isaksson et al., 2019). In any case, these values ensure the assessment of internal doses well below the reference level.

In particular, gamma cameras not only demonstrate excellent sensitivity but also high precision in activity quantification, with negligible dependence on the model used. The efficiency values and detection limits are highly consistent across different models and align well with findings from similar studies (Dantas et al., 2007) (Navarro et al., 2020).

Conversely, non-spectrometric devices exhibit lower sensitivity, with efficiency and detection limit values strongly dependent on the probe type and the counting time.

Finally, based on the results obtained in Phase I, it is confirmed that the calibration protocol has been performed correctly, and no corrections are required for its use in Phase II of the project. It has also been confirmed that spectrometric equipment and gamma cameras are highly suitable for screening tasks during the early stages of an emergency. Likewise, non-spectrometric devices are also suitable; however, prior data on their measurement sensitivity are necessary to determine their suitability for such scenarios.

CRediT authorship contribution statement

J.F. Navarro: Data curation, Formal analysis, Investigation, Methodology, Resources, Supervision, Validation, Visualization, Writing – original draft, Writing – review & editing. **B. Pérez:** Formal analysis, Investigation, Methodology, Resources, Software, Supervision, Validation, Writing – original draft, Writing – review & editing. **M.A. López:** Data curation, Formal analysis, Funding acquisition, Investigation, Methodology, Resources, Supervision, Writing – original draft, Writing – review & editing. **S. Pereira:** Methodology, Supervision, Visualization, Writing – review & editing. **J. Ruiz:** Formal analysis, Methodology, Resources, Software, Supervision, Validation, Writing – review & editing. **I. Sierra:** Methodology, Resources, Validation, Writing – review & editing. **D. Rueda:** Visualization, Writing – review & editing. **I. Villanueva:** Funding acquisition, Investigation, Resources, Supervision, Validation, Writing – review & editing.

Declaration of competing interest

The authors declare that they have no known competing financial interests or personal relationships that could have appeared to influence the work reported in this paper.

Table 6
DL/MDA (Bq) -Spectrometric devices.

DL/MDA (Bq) -Spectrometric devices										
EQUIPMENT/INSTITUTION	Tm(s)	CODE	Adult		10 y		5 y		1 y	
			10 cm	5 cm	10 cm	5 cm	10 cm	5 cm	10 cm	5 cm
BEGe detector CIEMAT	600	CIEMAT BEGe	12	6	9	5	7	4	6	3
HP Ge detector Univ. VALENCIA	900	UV HPGe	73	53	65	35	50	25	42	19
NaI (Tl(detector Univ. VALENCIA	900	UV NaI	317	141	156	91	134	58	102	45
NaI (Tl) detector Hosp. La Fe	300	LaFe NaI	198	93	272	87	179	97	183	103
LaBr3(Ce) detector Univ. País Vasco	300	UPV LaBr3	363	233	207	126	118	83	92	55
EQUIPMENT/INSTITUTION	Tm(s)	CODE	Adult		10 y		5 y		1 y	
			14 cm	25 cm	14 cm	25 cm	14 cm	25 cm	14 cm	25 cm
Quicky NaI counter TECNATOM	120	TEC_QUICKY	424		209		102		58	
FASTSCAN counter CIEMAT	300	CIEMAT_FS	81		74		72		63	
DIYS NaI counter TECNATOM (1)	480	TEC_DYIS	233		138		32		29	
CAPTUS2000 uptaker Hosp.San Pau	300	HSP CAPTUS		494		484		445		438

(1) DYS NaI. Detecto-phantom distance: d = 18 cm (adult), d = 19 cm (10y), d = 16.5 cm (5y), d = 14 cm (1y).

Table 7
DL/MDA (Bq) -Gamma cameras.

DL/MDA (Bq) -Gamma cameras									
EQUIPMENT/INSTITUTION	CODE	Adult		10y		5 y		1 y	
		10 cm	15 cm	10 cm	15 cm	10 cm	15 cm	10 cm	15 cm
Gamma camera Siemens Intevo Hosp. Santa Creu y San Pau	HSP siemens	41	54	41	55	37	49	36	49
Gamma camera Philips Brightview Hosp. Santa Creu y San Pau	HSP philips	47	63	45	63	42	58	36	53
Gamma camera Philips Brightview 1 Hosp. La Fe	HLaFe philips 1	48	59	47	62	44	57	39	54
Gamma camera Philips Brightview 2 Hosp. La Fe	HLaFe philips 2	49	63	46	60	44	60	42	57

Table 8
DL/MDA (Bq) –non-spectrometric devices.

DL/MDA (Bq) –non-spectrometric devices										
EQUIPMENT/INSTITUTION	Tm(s)	CODE	Adult		10y		5 y		1 y	
			10 cm	5 cm	10 cm	5 cm	10 cm	5 cm	10 cm	5 cm
BERTHOLD LB124 CIEMAT	120	CIEMAT LB124	352	190	321	176	251	152	155	120
BERTHOLD LB124 SCINT D Hosp.S.P.	150	HSP LB124	141	74	159	66	190	54	120	58
LAMSE, MS6020-R. Univ. Islas Baleares	600	UnivIB Lamse	154	73	163	79	192	58	207	56
Babyline 81. radiometer UNIV. País Vasco	60	UPV Babyline		6580		8041		9197		6414

Acknowledgements

This work was supported and funded by an agreement between CSN, CIEMAT, and the company TECNATOM to implement the R&D project MEYER (Towards a National Protocol for the Evaluation of ^{131}I in Emergency Situations) within the Spain's National R&D Platform for Radiological Protection (PEPRI).

Data availability

Data will be made available on request.

References

ANSI/HPS N13.44 2014 Edition, 2014. Thyroid Phantom Used in Occupational Monitoring.

Broggio, D., et al., 2019. Child and adult thyroid monitoring after a reactor accident (CAThyMARA): technical recommendations and remaining gaps. Radiat. Meas. 128, 106069. https://doi.org/10.1016/j.radmeas.2019.02.008. ISSN 1350-4487.

Dantas, B.M., et al., 2007. A protocol for the calibration of gamma cameras to estimate internal contamination in emergency situations. Radiat. Protect. Dosim. 127 (1–4), 253–257. https://doi.org/10.1093/rpd/ncm278.

ICRP, 2002. Basic anatomical and physiological data for use in radiological protection reference values. ICRP Publ. 89. Ann. ICRP 32 (3-4).

Isaksson, M., et al., 2019. Assessing ^{131}I in thyroid by non-spectroscopic instruments, A European intercomparison exercise. Radiat. Protect. Dosim. 128, 106115. https://doi.org/10.1016/j.radmeas.2019.04.018.

Navarro, J.F., et al., 2020. Calibration of a SPECT-CT gamma camera with child and adult thyroid-neck phantoms for in vivo monitoring of radioiodine in the exposed population in case of nuclear emergency. Radiat. Phys. Chem. 171, 108668. https://doi.org/10.1016/j.radphyschem.2019.108668. ISSN 0969-806X.

Pérez, B., Navarro, J.F., López, M.A., 2018. Methodology at Ciemat Whole Body Counter for in vivo monitoring of radioiodine in the thyroid of exposed population in case of nuclear emergency. Radiat. Protect. Dosim. 1–6. https://doi.org/10.1093/rpd/ncy045.

Pérez, B., Navarro, J.F., López, M.A., 2020. CIEMAT WBC capabilities for responding in case of nuclear and radiological emergencies. Radiat. Phys. Chem. https://doi.org/10.1016/j.radphyschem.2020.108977.

UNSCEAR 2013 Report. Vol 1. Anex A. Levels of effects of radiation exposure due to the nuclear accident after the 2011 great east Japan earthquake and tsunami. www.unscear.org/docs/reports/2013.